MULTISTABILITY OF PLATES THROUGH VARIABLE STIFFNESS COMPOSITE USING RAYLEIGH RITZ METHOD

Ayan Haldar[*]**, José Reinoso**[†]**, Eelco Jansen**[*]**, Raimund Rolfes**[*]

[*]Leibniz Universität Hannover

Institute of Structural Analysis,Appelstr. 9A,30167 Hannover, Germany
e-mail: a.haldar@isd.uni-hannover.de

[†]Universidad de Seville

Mechanics of Continuous Media and Theory of Structures, Seville, Spain
e-mail: jreinoso@us.es

Keywords: Multistability, Variable Stiffness Composites, Rayleigh Ritz, Morphing, Residual thermal stresses

Summary: Bi-stability was traditionally achieved in unsymmetrical laminates, where the angle of the fiber path was either constant or varied discretely in the plane of laminae. In this work, the multi-stable shapes of Variable Stiffness (VS) composites are investigated by means of semi-analytical approach. The concept of VS was introduced so the fiber can traverse the plane of the laminae with a continuous angle variation. Although, there are many possibilities of varying the fiber direction, in this paper a curvilinear fiber variation in plane is used for the ease of manufacturing. A suitable stiffness tailoring can be possible which results in easy morphing of the flexible part and load carrying capacity for the stiffer part. The semi-analytical approach is constructed using Rayleigh Ritz method which is implemented into the commercial package *Mathematica* where appropriate approximation functions for the displacement field are used in order to: (i) identify the multiple potential solutions (ii) perform the subsequent stability assessment of the obtained solutions. The analysis results provide a relation between the changing orientation of the fibers and the stable shapes obtained for different VS composite configurations. Parametric studies are further carried out to determine different stable shapes attained by changing fiber orientations. Finally, a comparison with the multistable shapes of straight fiber configurations stiffness laminates is performed.

1. INTRODUCTION

It was 18th century when the clock maker John Harrison [1] first devised one of the simplest morphing structures: the bimetallic strip. Due to the difference in the thermal coefficient in the two metals, heating lead to another curved stable configuration. Still, its widely used in thermostats, thermometers and circuit breaker. Later, Hyer [2] performed experiments on cooling of thin unsymmetrical laminates and had similar observations. On cooling down to room

temperature, two different stable cylindrical shapes were observed, which were quite different from what was predicted by classical lamination theory. One cylindrical configuration had a large curvature in x direction and an unnoticeable curvature in y direction, whereas the other cylindrical shape had a large curvature in y direction and an unnoticeable curvature in the x direction (Fig. 1). Classical lamination theory predicted that at the room-temperature shapes of all unsymmetrical laminates to be saddle. With inclusion of inclusion of geometrical nonlinearities [3], the numerical results revealed not just the two stable shapes but rather an additional unstable saddle shape, which is not captured in the experimental process.
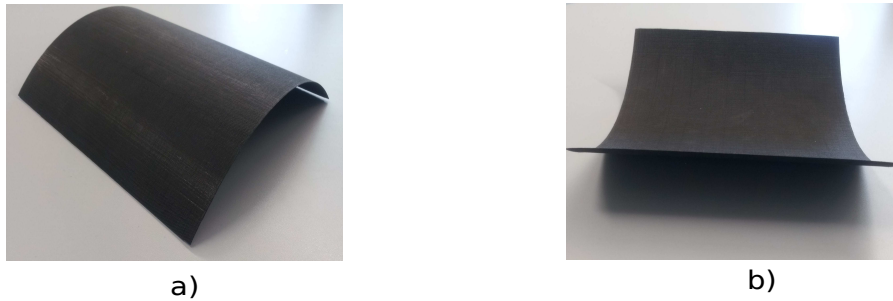

a)   b)

Figure 1. Cured shapes of unsymmetrical $[0/90]$ laminates (Experiment performed at ENS Cachan)

Relying on these pioneering works [2, 3], and other subsequent paper [4], the multistability of composite laminates has attracted a great deal of attention in the following years. Several researchers further contributed in refining the displacement interpolation space [5, 6, 7, 8]. In this regard, Dang and Tang [7] added more sophisticated polynomial terms in the displacement function, and later Jun and Jong [5] further used complex variables and trigonometric relations to simplify the expressions. It was Dano and Hyer [9] who came up with a new model where they assumed a strain field and derived the displacement field from it rather than a assuming the displacement field and working out the strains. The advantage was the obtained simplified terms in the final potential energy as the stresses and the strain field could directly be used in the total potential energy equation. This work is presently considered as state of art and is used in this paper to calculate the cured shapes.

Dano and Hyer [9, 10] introduced the effect of adding a external force on the one of the stable state to predict the snap through behavior to another stable state. They used shape memory alloys to general end forces producing moments that lead to snap through phenomenon. This was solved numerically by introducing force terms into Ritz minimization and the resulting nonlinear equations were solved numerically. This was one of the first attempts to use the multistable unsymmetrical laminate favorably as morphing structures. The interest in multistable structure since then has reinvigorated in the research community, as it presents very interesting applicability in morphing structures. One of the important advantages that distinguishes it from other morphing techniques is its ability to remain in equilibrium position even after the shape

change occurs. That means no external force is required to hold the shape of the structure. Just a snap through force is enough to change the shape from one configuration to another, which can be achieved using piezo-composites [11, 12, 13, 14] or shape memory alloys [9, 15].

In the last few years, this subject has received wider attention and significant amount of work has been done to show its potential in morphing applications, especially in the aerospace industry [16, 17, 18, 19, 20]. However, the inherent challenge in all these adaptive structure in real applications is the obvious trade-off: to be flexible enough to allow large structural changes and at the same time able to withstand external loading in a controlled manner. If taken a little historical perspective of morphing structures in aerospace industry, one can always see the relevance of bio-mimicry while designing such structures. Since the invention of airplane, efforts have been made to make use of variable geometry as well as material to enhance flight control more like a bird. Perhaps, it was not the wrong solution but quite ahead of its time.

Today, advanced technology has helped creating structures which was perhaps a dream few decades ago. The evolution of composites has taken a leap further in the aerospace industry, with the introduction to VS composites. Automated Fiber Placement(AFP) offers the capability to place the fibers in a curvilinear path over the area of the lamina. This ability to locally tailor the fiber orientation provides designer a much wider design space, and allows them to develop composites with optimal properties. One of the promising solutions that can help us achieve morphing structure with inherent contradiction of high load carrying capacity and high deformation abilities posed by morphing can be offered by VS composites. Though there are manufacturing constraints with angles with sudden variations, but still offers huge design option than conventional straight fibers.

VS composite similar to those of unsymmetric straight fiber laminates exhibits multistable shapes when cured from high temperature to room temperature [21]. This can be used in much larger structures where only certain part could be made of unsymmetrical laminates to impart bi-stability along with ensuring fiber continuity. Panesar et al. [22] used bistable tow steered blended laminate to study the behavior of the stable states in trailing edge flap, and also found the optimum fiber direction for maximum out of plane displacement and maximum angle of attack. In the optimal results, it was seen that every discrete part of the flap should have a different values of fiber orientation. Mattioni [20] used a rectangular section comprising half of it as symmetric laminate and the other half as unsymmetrical laminate, though with straight fibers. This idea was implemented keeping in mind that it could be used as morphing parts in aerospace structure, where only certain part of the structure is needed to be adaptive. Though this model had interesting results, but because of fiber discontinuity lead to stress concentration at the point where the symmetric and the unsymmetrical plates were joined. A similar model was made by Sousa et al. [23], but instead of using discrete straight fibers, a much smoother fiber continuity was maintained by using curvilinear fiber trajectories. The geometry of the curing shapes was obtained by using a simplified finite element model. According to the knowledge of the authors, this is the only work where the multistability of VS laminates have been studied in detail, though an analytical formulation have not performed yet.

The present paper therefore aims at building a semi-analytic model for VS laminates based

on Rayleigh Ritz method, to find the thermally induced multistable shapes. The paper builds on the kinematics given by Dano and Hyer [9] with fiber path defined in Gürdal et al. [24]. The theory is then described to incorporate curvilinear fiber trajectories into the Rayleigh Ritz formulation to obtain the room temperature shapes. Next, the numerical results for a number of VS laminates are shown, and discussed in detail. The bending and twisting curvatures of various VS laminates are compared with the one with straight fibers.
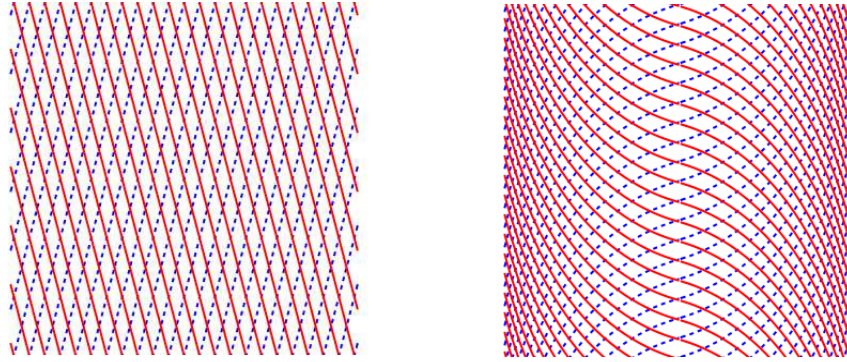

Figure 2. Comparison between straight fiber and variable stiffness fiber configuration

2. Variable Stiffness Laminates

Gurdal and Olmedo [25] defined the fiber orientation with linear variation of angle from the center to the end of the plate. Based on this, they performed closed form solution for buckling analysis due to in-plane forces. Later, Waldhart [26] showed that using VS panels, the buckling performance could be increased due to stiffness variation. Gürdal and Tatting [24] showed that using for a particular buckling critical load, there might exist a lot of possibilities with different VS composites, thus allowing a designer to a have more room for tailoring the stiffness and the same time the critical load of the structure. Figure 2 compares side by side a composite with straight fibers and the other with varying fiber orientation. It can be very clearly seen that stiffness is constant throughout the plate for a traditional straight fiber layup, whereas the concentration of the fibers is more towards the end for the VS laminates, thus leading to higher stiffness at the ends. These differences in the fiber orientation can lead to different stiffness properties and thus different structural behavior. Therefore, allowing the fibers can offer multiple advantages. It must be also noted that this change in fiber orientation can also lead to alteration of principle load paths, which can be interesting for morphing structures where the load can be altered toward stiffer part allowing the flexible part to undergo large deformations.

2.1 Fiber path definition

There are several ways to vary the fiber angle however, due to manufacturing constraints, a linear variation of fiber orientation as proposed by [24] is used in this paper. It is defined as:
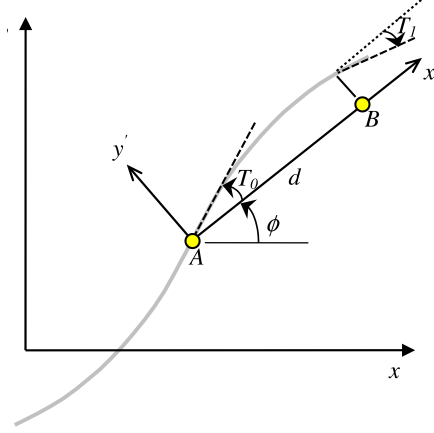
Figure 3. Parameters that define linear fiber angle variation [24]

$$\theta(x') = \begin{cases} \phi + \frac{2}{a}\left(T_1 - T_0\right)x' + T_0 - 2\left(T_0 - T_1\right), & \text{for } -a \le x \le -a/2 \\ \phi + \frac{2}{a}\left(T_0 - T_1\right)x' + T_0, & \text{for } -a/2 \le x \le 0 \\ \phi + \frac{2}{a}\left(T_1 - T_0\right)x' + T_0, & \text{for } 0 \le x \le a/2 \\ \phi + \frac{2}{a}\left(T_0 - T_1\right)x' + T_0 - 2\left(T_0 - T_1\right), & \text{for } a/2 \le x \le a \end{cases} \tag{1}$$

where $x' = x\cos\phi + x\sin\phi$

The fiber goes from orientation angle T_0 at Point A to Point B at a distance d where the orientation angle linearly varies to T_1. The distance d is referred as the characteristic length (Fig. 3). The local coordinate axes x' and y' is rotated by angle ϕ with respect to the Cartesian coordinate axes. Fiber orientation is considered to be symmetric along $x = 0$. In this work, square plates have been used throughout and thus the characteristic length d is equal to half the length of the plate ($a/2$). Therefore, T_0 is the fiber orientation at $x = 0$ and T_1 at the plate end, $x = \pm a/2$ where a is the length of the plate. This linear variation of fiber orientation is given by Eq. (1). Although the fiber is changing its orientation along x' direction, if seen from the reference of x and y axes, the fiber orientation is a function of x and y: $\theta = \theta(x, y)$.

Through the parameters defined above, different kinds of VS fiber orientation can be defined. The standard notation to depict a VS laminate using the three parameters is: $\phi\langle T_0|T_1\rangle$. One can construct laminates by the combination of ϕ and $\pm\langle T_0|T_1\rangle$. For example in $\pm\phi \pm \langle T_0|T_1\rangle$ laminate, the composite has in total 8 layers, with four layers $\pm\langle T_0|T_1\rangle$ oriented in $+\phi$ direction and the other four laminates oriented in $-\phi$ direction. $\pm\langle T_0|T_1\rangle$ depicts adjacent layers with $+\langle T_0|T_1\rangle$ and $-\langle T_0|T_1\rangle$ fiber orientation angles. Fig. 2 shows an example of a VS composite with a configuration: $\pm\langle 15|75\rangle$. In case of structures with unequal aspect ratio, the fiber definition can be further extended with similar pattern as shown in Eq. (1).

2.2 Theoretical Approach: Extended Classical Lamination Theory

The semi-analytical model used in this paper is based on the Rayleigh Ritz model using the Extended Classical Lamination theory (ECLT), where the nonlinear Von Kármán strains are used to incorporate large deflections. Here, ECLT is used to determine the multistable shapes of the VS composite when cured from a high temperature to room temperature. In this work, a square plate of length L_x is considered with thickness t. No external mechanical forces and hygroscopic effects are been considered and therefore the total potential energy of the laminate is equals to the strain energy. It should be also noted that as the fiber orientation is a function of x and y, the ABD matrix also varies along the coordinates of the plate. This flexibility to change the stiffness terms of a plate as a function of the coordinates of the composite allows a designer to have a wide range of tailoring possibilities. The following set of equations systematically derive the total potential energy from an assumed polynomial displacement field. The kind of displacement field chosen is discussed in the next section (Section 2.3).

$$u(x,y,z) = u_0(x,y) - z\frac{\partial w_0}{\partial x}, \;\; v(x,y,z) = v_0(x,y) - z\frac{\partial w_0}{\partial y}, \;\; w(x,y,z) = w_0(x,y) \quad (2)$$

where the subscript 0 identifies the mid-plane displacements. u, v and w represents the displacements in x, y and z direction respectively. In case of small strains and small rotations, the strain components take the form:

$$\epsilon_{xx} = \frac{\partial u}{\partial x} + \frac{1}{2}\left(\frac{\partial w}{\partial x}\right)^2, \;\; \epsilon_{yy} = \frac{\partial v}{\partial y} + \frac{1}{2}\left(\frac{\partial w}{\partial y}\right)^2, \;\; \gamma_{xy} = \frac{\partial u}{\partial y} + \frac{\partial v}{\partial x} + \frac{\partial w}{\partial x}\frac{\partial w}{\partial y} \quad (3)$$

By inserting (3) into (2), the strain relations can be rearranged as

$$\boldsymbol{\epsilon} = \begin{bmatrix} \epsilon_{xx} \\ \epsilon_{yy} \\ \gamma_{xy} \end{bmatrix} = \begin{bmatrix} \varepsilon_{xx} \\ \varepsilon_{yy} \\ \varepsilon_{xy} \end{bmatrix} + z\begin{bmatrix} \kappa_{xx} \\ \kappa_{yy} \\ \kappa_{xy} \end{bmatrix} = \begin{bmatrix} \frac{\partial u_0}{\partial x} + \frac{1}{2}\left(\frac{\partial w_0}{\partial x}\right)^2 \\ \frac{\partial v_0}{\partial y} + \frac{1}{2}\left(\frac{\partial w_0}{\partial y}\right)^2 \\ \frac{\partial u_0}{\partial y} + \frac{\partial v_0}{\partial x} + \frac{\partial w_0}{\partial x}\frac{\partial w_0}{\partial y} \end{bmatrix} + z\begin{bmatrix} -\frac{\partial^2 w_0}{\partial x^2} \\ -\frac{\partial^2 w_0}{\partial y^2} \\ -2\frac{\partial^2 w_0}{\partial x \partial y} \end{bmatrix} = \boldsymbol{\varepsilon} + z\boldsymbol{\kappa}, \quad (4)$$

where $\boldsymbol{\varepsilon}$ and $\boldsymbol{\kappa}$ represent the in-plane and curvature vectors. The constitutive law for each layer k that composes the laminate taking into account the thermal effects in the global Cartesian frame reads as:

$$\boldsymbol{\sigma} = \begin{bmatrix} \sigma_{xx} \\ \sigma_{yy} \\ \sigma_{xy} \end{bmatrix}^{(k)} = \begin{bmatrix} Q_{11}(x,y) & Q_{12}(x,y) & Q_{16}(x,y) \\ Q_{12}(x,y) & Q_{22}(x,y) & Q_{26}(x,y) \\ Q_{16}(x,y) & Q_{26}(x,y) & Q_{66}(x,y) \end{bmatrix}^{(k)} \left(\begin{bmatrix} \epsilon_{xx} \\ \epsilon_{yy} \\ \gamma_{xy} \end{bmatrix} - \Delta T \begin{bmatrix} \alpha_{xx} \\ \alpha_{yy} \\ 2\alpha_{xy} \end{bmatrix}^{(k)} \right) \quad (5)$$

Note that in (5), the constitutive matrix is a function of x and y. Integrating over the thickness the stress-strain relation, it is possible to rewrite (5) in terms of the force and moments resultants.

$$\begin{bmatrix} \mathbf{N}(x,y) \\ \mathbf{M}(x,y) \end{bmatrix} = \begin{bmatrix} \mathbf{A}(x,y) & \mathbf{B}(x,y) \\ \mathbf{B}(x,y) & \mathbf{D}(x,y) \end{bmatrix} \begin{bmatrix} \boldsymbol{\varepsilon} \\ \boldsymbol{\kappa} \end{bmatrix} - \begin{bmatrix} \mathbf{N}^{th}(x,y) \\ \mathbf{M}^{th}(x,y) \end{bmatrix} \quad (6)$$

In (6), the resultant quantities with the superscript th denotes the thermal actions. As, the Q matrix is a function of x and y, coordinate, but independent of the z coordinate $\mathbf{A}$, $\mathbf{B}$ and $\mathbf{D}$ matrix was simply calculated as:

$$
A_{ij}(x,y) = \sum_{k=1}^{N_{ply}} Q_{ij}^{(k)}(x,y)\,(z_{k+1} - z_k)\,, \ B_{ij}(x,y) = \frac{1}{2}\sum_{k=1}^{N_{ply}} Q_{ij}^{(k)}(x,y)\,(z_{k+1}^2 - z_k^2)
$$
$$
D_{ij}(x,y) = \frac{1}{3}\sum_{k=1}^{N_{ply}} Q_{ij}^{(k)}(x,y)\,(z_{k+1}^3 - z_k^3) \tag{7}
$$

The response of the laminated structure is determined by means of the Minimum Potential Energy Theorem. The potential energy of the structure in absence of external mechanical actions is given by

$$
\Pi = \int_{-L_x/2}^{L_x/2}\int_{-L_y/2}^{L_y/2}\left(\frac{1}{2}\begin{bmatrix}\boldsymbol{\varepsilon}\\ \boldsymbol{\kappa}\end{bmatrix}^T\begin{bmatrix}\mathbf{A}(x,y) & \mathbf{B}(x,y)\\ \mathbf{B}(x,y) & \mathbf{D}(x,y)\end{bmatrix}\begin{bmatrix}\boldsymbol{\varepsilon}\\ \boldsymbol{\kappa}\end{bmatrix} - \begin{bmatrix}\mathbf{N}^{th}(x,y)\\ \mathbf{M}^{th}(x,y)\end{bmatrix}^T\begin{bmatrix}\boldsymbol{\varepsilon}\\ \boldsymbol{\kappa}\end{bmatrix}\right)\ \mathrm{d}x\,\mathrm{d}y \tag{8}
$$

where the superscript T denotes vector transpose. The Rayleigh-Ritz method can be applied using (8) as starting point, minimizing the potential energy of the structure ($\delta\Pi = 0$). The displacements will depend upon a certain number of unknowns denoted as c_i (i = 1, nn being the total number of unknowns) that need to be determined. Then, plugging the dependency of the kinematic field on these unknowns into (8), one may express the strain energy as:

$$
\Pi \approx \Pi_N(\mathbf{c}),\ \ \mathbf{c} = \{c_i\},\ \text{i=1, ..., nn} \tag{9}
$$

The strain energy expressed in (9) corresponds to an algebraic equation in terms of the set of variables $\mathbf{c}$ used for the kinematic approximation (where nn refers to the number of parameters considered). Therefore, the equilibrium configurations of the panel are determined by satisfying $\nabla\Pi_N(\mathbf{c}) = \mathbf{0}$, which leads to the establishment of a set of nonlinear equations.

The stability of the solution is evaluated by means of the construction of the Jacobian matrix $\mathbf{J}$, that reads:

$$
\mathbf{J} = \frac{\partial^2\Pi_N}{\partial c_i \partial c_j},\, \text{i,j=1, ..., nn} \tag{10}
$$

Hence, an equilibrium configuration is stable if and only if the corresponding Jacobian matrix (10) is positive definite, and is unstable otherwise. In the context of the present investigation, the total potential energy of the plate, its symbolic differentiation and the construction of the Jacobian matrix have been conducted using the software *Mathematica*. The system of nonlinear equations (9) are solved using the function *NSolve* and the stability criterion introduced in (10) can be computed using the function *PositiveDefiniteMatrixQ*. At every temperature increment, the matrix $\mathbf{J}$ is computed and checked for its stability.

2.3 Kinematics

In the related literature, several models have been proposed for the multi-stability analysis of composite speciments along the cooling down process from curing to room temperature. Since Hyer [3], several researchers have worked in refining the semi-analytical model for exact solutions. In this quest, many of those authors have come up with quite a number of models ranging from quite simple approximations to higher order polynomials. Reinoso et al. [27] have compared the results given by some of the available established models with Finite Elements and have discussed the robustness and accuracy.

The curvatures of the resulting stable solution can be identified from the coefficient of the out of plane displacement function. The number of unknowns and the approximation used greatly effects the accuracy of the results obtained. For example, one of the initial models by Hyer [3], defines the displacement function as where $w_0 = \frac{1}{2}(c_3 x^2 + c_4 y^2)$, c_3 identifies the curvature along the x-direction and c_4 denotes the curvature along the y-direction. It can be seen that the curvatures are predicted to have a constant value throughout the structure, though no twisting behavior is included in the model. Dang and Tong [7] included twisting terms by adding more polynomial terms, though ending up in quite complex polynomial functions and used trigonometric relations to reduce the number of unknowns. Dano and Hyer [9] incorporated both the bending in x and y direction (κ_x and κ_y) as well as a twisting component (κ_{xy}) in a very simple fashion without involving quite higher complex displacement expressions.

In case of VS composites, as a consequence of their complex conceptions, they can undergo twisting curvatures, and therefore it is important to include reliable approximation function that can capture these effects in a simple and reliable fashion. Therefore, in this work, the kinematic field proposed by Dano and Hyer [9] is considered. Though the model, both the bending curvatures and the twisting curvature can be well captured. Wu [21] also also confirmed through experimental data asymmetric VS laminates when cured from high to room temperature exhibits close to cylindrical shapes.

The mid-plane strains are approximated as the following set of complete polynomials:

$$\varepsilon_x^0 = c_1 + c_2 x^2 + c_3 y^2 + c_4 xy \tag{11}$$

$$\varepsilon_y^0 = c_5 + c_6 x^2 + c_7 y^2 + c_8 xy \tag{12}$$

The out of plane displacement is approximated as:

$$w_0(x,y) = \frac{1}{2}(c_9^2 + c_{10} y^2 + c_{11} xy) \tag{13}$$

The coefficients from c_1 to c_{11} are the set of unknowns need to be determined. c_9, c_{10} and c_{11} are nothing but the negative curvature in x and y directions and the negative twist curvature.

$$\kappa_{xx} = \frac{\partial^2 w_0}{\partial x^2} = -c_9, \ \kappa_{yy} = \frac{\partial^2 w_0}{\partial y^2} = -c_{10}, \ \kappa_{xy} = 2\frac{\partial^2 w_0}{\partial x \partial y} = -c_{11} \tag{14}$$

Analyzing (14, it is quite evident that the curvatures are considered constant. However, Mattioni et al. [20] used non uniform curvatures to model multistable structure where symmetric and unsymmetrical laminates are joined together and thus doesn't have a free edge boundary condition. Such calculations increase the number of coefficient and solving nonlinear system of equation in the Rayleigh Ritz framework can be difficult.

Using Eq. (13) in the expression for extensional strains ε_x^0 and ε_y^0 (Eq (11)) one can compute the in-plane displacements:

$$u_0(x, y) = \int \left[\varepsilon_x^0 - \frac{1}{2} \left(\frac{\partial w^0}{\partial x} \right)^2 \right] dx + c_{12}y + c_{13}y^3 \tag{15}$$

$$v_0(x, y) = \int \left[\varepsilon_y^0 - \frac{1}{2} \left(\frac{\partial w^0}{\partial y} \right)^2 \right] dy + c_{15}x + c_{14}x^3 \tag{16}$$

$$\tag{17}$$

Here additional unknowns c_{12}, c_{13}, c_{14} and c_{15} are needed to be solved too. In order to remove rigid body motion from the assumed displacement field, the first order terms of the variable x and y are needed to be equated, which results in $c_{15} = c_{12}$. The shear strain can be simply calculated from the equation below:

$$\gamma^0 = \frac{\partial u^0}{\partial y} + \frac{\partial v^0}{\partial x} + \frac{\partial w^0}{\partial y} \frac{\partial w^0}{\partial x} \tag{18}$$

3. RESULTS

The geometry and material of plate is chosen taking into consideration the model by Dano and Hyer [9] where the size of the plate is taken as 11.5×11.5 in^2 and total thickness of the laminate as 0.040; in. The material properties of a layer of graphite-epoxy were considered as:

$$E_1 = 27.77 \times 10^6 \text{ psi}, \ E_2 = 1.27 \times 10^6 \text{ psi}, \ G_{12} = 1.03 \times 10^6 \text{ psi}$$
$$\nu_{12} = 0.335, \ \alpha_1 = 0.345 \times 10^{-6}/°F, \ \alpha_2 = 15.34 \times 10^{-6}/°F \tag{19}$$

Specific details concerning the VS composite and the straight fiber configuration herein analyzed are given in Table 1. Here the composite consists of eight layers, where the fiber varies from $+T_0$ value from the center to $+T_1$ at the edges for the first four layers, and the next four layer $-T_0$ in the center to $-T_1$ at the edges, making it an unsymmetric composite. As discussed in Section 2.2, after all the unknowns ($c_1..c_{14}$) are found using Rayleigh Ritz, it is substituted back to Eq. (11) to Eq. (13) to obtain the displacement fields, and the curvatures of the cured shape.
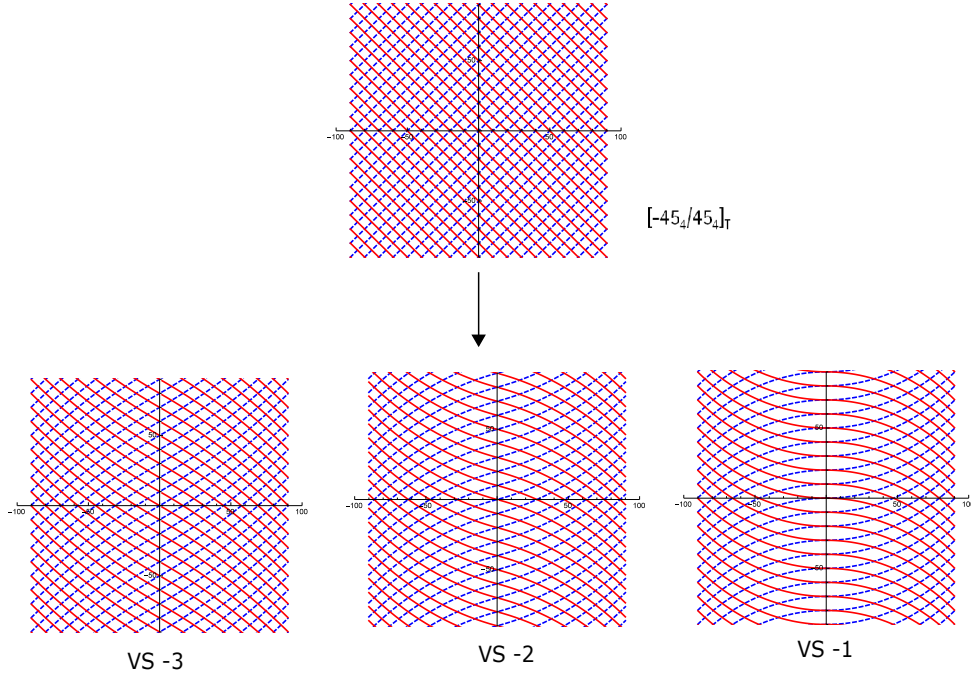
Figure 4. Fiber orientation of the numerical example

Type	ϕ	T_0	T_1	Layup
VS-1	0	± 0	± 45	$[0\langle 0|45\rangle_4/0\langle 0| - 45\rangle_4]_{\mathrm{T}}$
VS-2	0	± 15	± 45	$[0\langle 15|45\rangle_4/0\langle -15| - 45\rangle_4]_{\mathrm{T}}$
VS-3	0	± 30	± 45	$[30\langle 0|45\rangle_4/0\langle -30| - 45\rangle_4]_{\mathrm{T}}$
Straight	0	± 45	± 45	$[-45_4/45_4]_{\mathrm{T}}$

Table 1. Fiber orientation and layup data for the VS and straight laminates

3.1 Room temperature configurations for variable stiffness composite

In this section, the multistable shapes for the VS composite found out are discussed in detail. All the VS laminates are constructed on the basis of straight fiber configuration: $[-45_4/45_4]_{\mathrm{T}}$. As shown in the Table 1, the value of fiber orientation at the edge of plate i.e. T_1 is taken as $\pm 45°$ for all the VS laminates studied, which is equal to the fiber orientation of the straight fiber laminate. The fiber orientation from the center of the plate to the end varies significantly for all the VS laminates. As seen in Figure 4, the value of fiber orientation for VS-1 varies from $0°$ at the center to $45°$ at the edge. Similar, for VS-3, the value of fiber orientation for VS-1 varies from $0°$ at the center to $45°$ at the edge. It can be seen that the amount of fiber steering increases from VS-3 to VS-1. Extreme deviations are not taken in this study as such fiber orientation pose difficulty in manufacturing process.

It is also interesting to note how the stiffness of the plate varies on changing the three param-

eters needed to define VS composites. For example, in VS-1 the fibers are more concentrated at the edges and density of fibers is quite less in the center. This amount of freedom to tailor the stiffness plays an important role in obtaining multistable structure with different structural behavior.

The curvature- temperature relationship obtained from the developed theory for each VS composite are illustrated in Fig.5. The straight fiber results are obtained simply by putting the values of T_0 and T_1 equal, in this case ($\pm 45°$). The values obtained are also validated with the model with straight fibers by Dano and Hye [9].

In Fig. 5, the important points are marked as A, B, C, D and E. All these points are marked for the straight fiber laminate. However, the phenomenon occurring at these points can be seen as well for the VS laminates. The labeling of these points for all the VS laminates are not done to avoid cluttering.

Point A (stress free state) depicts the curing temperature, where the temperature difference from the room temperature is $280°$F, and at this point the plate is considered flat. With slight cooling down, it is seen that twisting curvature κ_{xy} begins to develop while the bending curvatures (κ_x, κ_y) still remain zero. As the temperature is decreased further to point B, the bifurcation point is encountered. From this point, the structure follows either of the paths: BC, BE or BD.

In Fig. 5, the points near the bifurcation points for all the laminates have been zoomed to give a better illustration of the phenomenon. It can be seen that the bifurcation point occurs later for all the VS laminates. In case of VS-3, the bifurcation point ($\Delta T \approx 40°$F) is quite near to bifurcation point of straight fiber configuration ($\Delta T \approx 35°$F). For VS-1 laminate, the bifurcation occurs much later ($\Delta T \approx 104°$F), and till that state only twisting curvatures are developed.

Point C and D refers to the stable equilibrium states, and for $T_1 = \pm 45°$, both path BC and BD are similar. In case of the plot between κ_x and ΔT, it is interesting to note that VS-3 which has $T_0 = \pm 30$, attains more curvature than the straight fiber laminate once it reaches the room temperature. Both of them have the same κ_x at around $190°$F, but the rate of κ_x is higher for VS-3. For other VS laminates, the curvature increases in a much slower rate, and develops smaller curvature in room temperature.

Dano [28] have showed for the family of $[-\theta_4/\theta_4]$ in straight fiber laminates, the values of κ_x and κ_y are equal with $\theta = \pm 45°$, but other fiber orientation tends to have unequal values of κ_x and κ_y. Unlike the straight fiber $[-45_4/45_4]$, the VS laminates have unequal values of κ_x and κ_y. It can be seen from the figure 5 that the rate of curvature for VS-3 and VS-2 are higher than the straight fiber. After the cool down to room temperature, for all the VS laminates addressed have curvature in y direction (κ_y) more than the curvature in x direction (κ_x). The reason for such behavior can be explained by variation of coefficient of thermal expansion (CTE) in x and y direction due to different fiber orientations. In order to understand this behavior let's see first
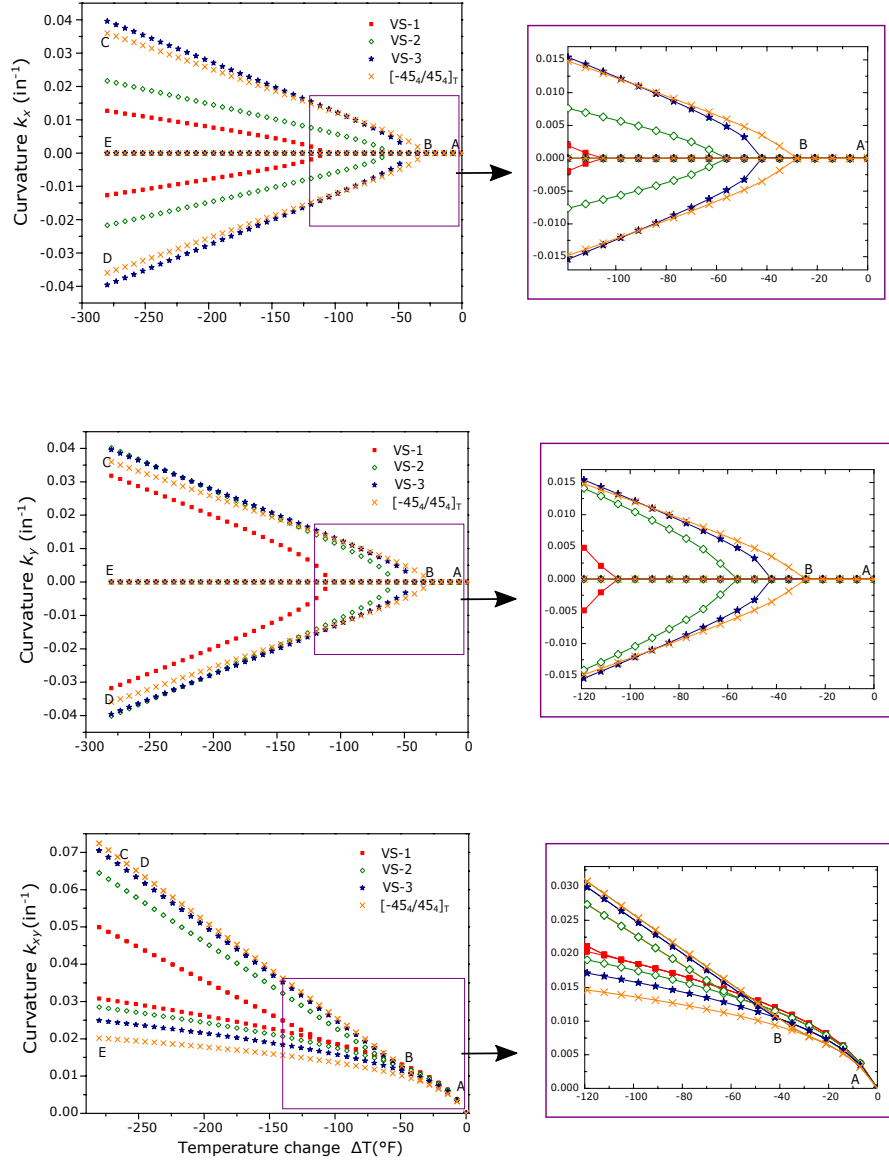
11

Figure 5. Temperature-curvature relationship for various VS laminates and a straight laminate, right hand side shows the zoomed version near the bifurcation point

how the CTE varies with fiber angles:

$$\overline{\alpha}_{xx} = \alpha_{11}\cos^2\theta + \alpha_{22}\sin^2\theta \tag{20}$$

$$\overline{\alpha}_{yy} = \alpha_{11}\sin^2\theta + \alpha_{22}\cos^2\theta \tag{21}$$

$$\overline{\alpha}_{xy} = 2\sin\theta\cos\theta(\alpha_{11} - \alpha_{22}) \tag{22}$$

12
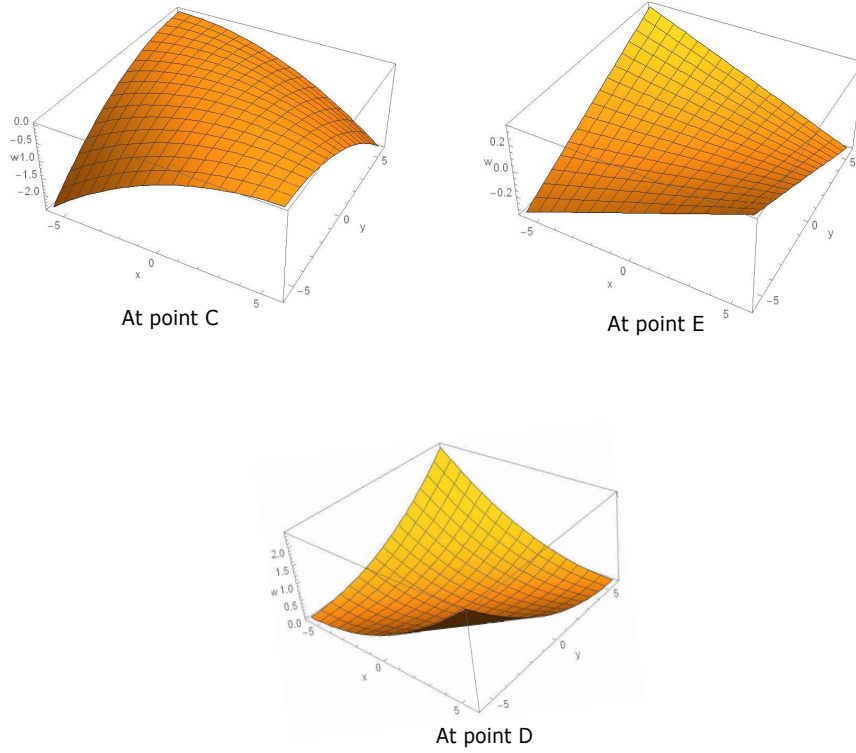
At point C

At point E

At point D

Figure 6. Stable and unstable shapes of VS-3 laminate at room temperature

In our study, as all the VS laminates hold the condition $T_0 < T_1$, which means that fiber angles are decreasing from edge to center. Therefore, we can say the $\cos\theta$ component is the one increasing from edge of the plate to center, for VS laminate. So, the value of $\overline{\alpha}_{xx}$ is primary increased in the layer by the component $\alpha_{11}\cos^2\theta$ and the value of $\overline{\alpha}_{yy}$ by $\alpha_{22}\cos^2\theta$. As, the value of $\alpha_{22} > \alpha_{11}$, the difference in the coefficient of thermal expansion is more in the y direction, leading to higher curvatures values κ_y for VS composites.

Point E represents the curvature at room temperature for the unstable equilibrium, which is never observed in experiments. With path BE, the curvature in the x and y axis remains zero for straight as well VS laminates. However, there is non-zero twist curvature developed though the rate of curvature increase is much smaller than the other two stable paths.

Figure 6 shows all the multistable shapes for VS laminate: VS-3. The other laminates have similar shapes with just with different magnitude, and thus not shown separately. Figure 7(a) compares the out of plane displacement with x coordinate over the plane $y = 0$ and Figure 7(b) compares the out of plane displacement with y coordinates over the plane $x = 0$. This gives a clear picture of how the out of plane displacement varies along the x and y axis in different VS composites. It can be seen that with decrease in T_0 values, the final out of plane displacement also reduces at the plane $y = 0$. It is interesting to note that the final out of plane displacement values for the VS-2 laminates are higher than the straight fiber laminate at the plane $x = 0$. Both the stable shapes are seen to have the same out of plane displacement at the plane $x = 0$

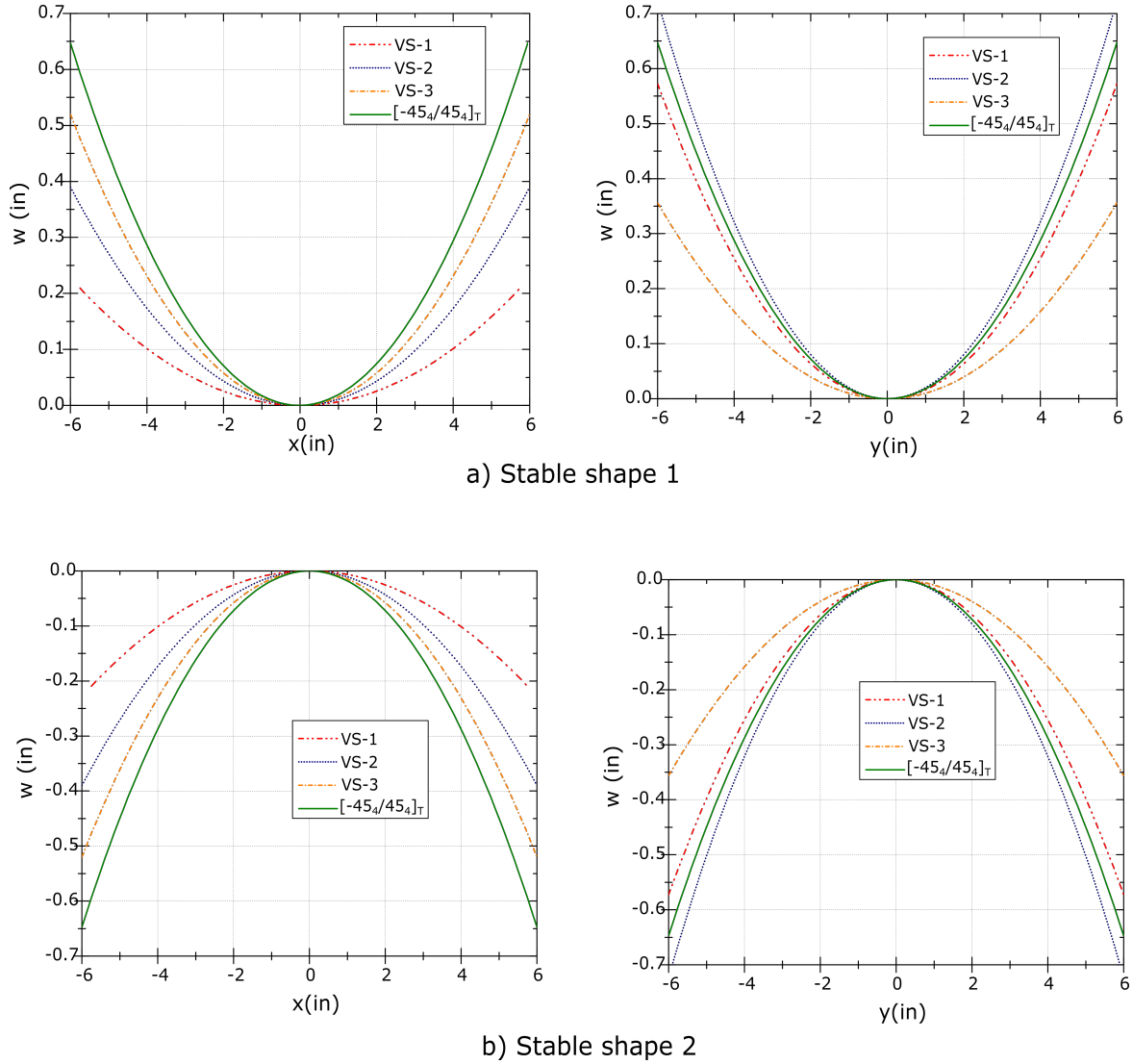a) Stable shape 1

b) Stable shape 2

Figure 7. Comparison of out of plane displacement of VS laminates and straight laminate at $x = 0$ and $y = 0$: a) Stable state 1 and b) Stable state 2

and $y = 0$ with just opposite curvatures.

4. CONCLUSION

In this work, a theory to predict the multistable shapes for VS composite is presented. The framework of the theory is based on the Extended Classical Lamination Theory (ECLT), which assumes in-plane strains and out of plane displacement fields with polynomial functions, and uses the Rayleigh Ritz method to calculate the unknowns of the strain fields and the displacement field. The fiber angle of the VS composite used in this work is assumed to vary linearly from the center of the plate to the edge. It is interesting to note that with decrease in temper-

ature, the VS laminates produced more curvatures in y direction than x direction ($\kappa_y > \kappa_y$). The reason was explained with how the coefficient of thermal expansion depends on the fiber orientation angle. Before the bifurcation point was reached, the VS laminates is seen to have only twisting curvatures. It was seen that with decrease in fiber orientation angle at the center lead to decrease in the out of plane displacement at the section $y = 0$. It was also noted that at the plane $x = 0$, the final out of the plane displacements were higher than the straight fiber configuration. After the bifurcation point, there were three possible branches, in which two of them were stable and other unstable. Shapes of both the stable shapes were similar with opposite curvatures. For all the VS laminates, the bifurcation point occurred much later than the straight fibers. The ΔT at which bifurcation occurred was maximum for $T_0 = 0°$ and reduced with increase in T_0.

Despite the lack of experimental results for a thermal curing process of an unsymmetric VS laminates, the results reported seems quite interesting and encouraging for further research. It would be interesting to see how the finite element results look now that the semi-analytical formulation has been made. Finite Element analysis would only produce the stable shape, when an initial imperfection is imposed into the model. The determination of such imperfection lies in qualitative information derived from the semi-analytical analysis.

It is also important to note that Rayleigh Ritz being analytic in nature provides a global sense of the structural behavior, and can be used as good approximate solution for complex geometries. However, local phenomenon occurring like the effect near the edges or corner might not be so accurately modeled using Rayleigh Ritz. For more complex geometries and material properties, finite elements can be suitable option once we have estimation of the multistable shapes found using the semi-analytical theory presented in this paper.

References

[1] D. Sobel. *Longitude*. London:Fourth Estate, 1995.

[2] M. W. Hyer. Some Observations on the Cured Shape of Thin Unsymmetric Laminates. *Journal of Composite Materials*, 15(2):175–194, 1981.

[3] M. W. Hyer. The Room-Temperature Shapes of Four-Layer Unsymmetric Cross-Ply Laminates. *Journal of Composite Materials*, 16(4):318–340, January 1982.

[4] Hamamoto Akira and M. W. Hyer. Non-linear temperature-curvature relationships for unsymmetric graphite-epoxy laminates. *International Journal of Solids and Structures*, 23(7):919–935, January 1987.

[5] W.J. Jun and C.S. Hong. Cured Shape of Unsymmetric Laminates with Arbitrary Lay-Up Angles. *Journal of Reinforced Plastics and Composites*, 11(12):1352–1366, December 1992.

[6] W.J. Jun and C.S. Hong. Effect of residual shear strain on the cured shape of unsymmetric cross-ply thin laminates. *Composites Science and Technology*, 38(1):55–67, 1990.

[7] Tang Y. Dang, J. Calculation of the room-temperature shapes of unsymmetric laminates. In *Proceedings of International Symposium on Composite Materials and Structures, Beijing, People's Republic of China, pp. 201–206*, 1986.

[8] M. Schlecht, K. Schulte, and M. W. Hyer. A comparative study for the calculation of the temperature dependent shapes of unsymmetric laminates based on finite element analysis and extended classical lamination theory. *Mechanics of Composite Materials*, 31(3):247–254, 1995.

[9] M Dano and M. W. Hyer. Snap-through of unsymmetric fiber-reinforced composite laminates. 39, 2002.

[10] Marie-Laure Dano and M. W. Hyer. the Response of Unsymmetric Laminates To Simple Applied Forces. *Mechanics of Advanced Materials and Structures*, 3(1):65–80, 1996.

[11] Marc R. Schultz, Michael W. Hyer, R. Brett Williams, W. Keats Wilkie, and Daniel J. Inman. Snap-through of unsymmetric laminates using piezocomposite actuators. *Composites Science and Technology*, 66(14):2442 – 2448, 2006. Special Issue in Honour of Professor C.T. Sun.

[12] Pedro Portela, Pedro Camanho, Paul M. Weaver, and Ian Bond. Analysis of morphing, multi stable structures actuated by piezoelectric patches. *Computers & Structures*, 86(3-5):347–356, February 2008.

[13] Samer A. Tawfik, D. Stefan Dancila, and Erian Armanios. Unsymmetric composite laminates morphing via piezoelectric actuators. *Composites Part A: Applied Science and Manufacturing*, 42(7):748–756, July 2011.

[14] C. R. Bowen, R. Butler, R. Jervis, H. a. Kim, and a. I. T. Salo. Morphing and shape control using unsymmetrical composites. 18(January), 2007.

[15] M.-L. Dano and M.W. Hyer. SMA-induced snap-through of unsymmetric fiber-reinforced composite laminates. *International Journal of Solids and Structures*, 40(22):5949–5972, November 2003.

[16] Cezar G. Diaconu, Paul M. Weaver, and Filippo Mattioni. Concepts for morphing airfoil sections using bi-stable laminated composite structures. *Thin-Walled Structures*, 46(6):689–701, June 2008.

[17] On a bistable flap for an airfoil. In *Collection of Technical Papers - AIAA/ASME/ASCE/AHS/ASC Structures, Structural Dynamics and Materials Conference*, 2009.

[18] F. Mattioni, P. M. Weaver, K. D. Potter, and M. I. Friswell. Analysis of thermally induced multistable composites. *International Journal of Solids and Structures*, 45(2):657–675, 2008.

[19] M. R. Schultz. A Concept for Airfoil-like Active Bistable Twisting Structures. *Journal of Intelligent Material Systems and Structures*, 19(2):157–169, 2007.

[20] F. Mattioni, Paul M. Weaver, and M.I. Friswell. Multistable composite plates with piecewise variation of lay-up in the planform. *International Journal of Solids and Structures*, 46(1):151–164, January 2009.

[21] Kinsley Chauncey Wu. *Thermal and Structural Performance of Tow-Placed, Variable Stiffness Panels*. IOS Press, 2006.

[22] Ajit S. Panesar and Paul M. Weaver. Optimisation of blended bistable laminates for a morphing flap. *Composite Structures*, 94(10):3092–3105, October 2012.

[23] C.S. Sousa, P.P. Camanho, and a. Suleman. Analysis of multistable variable stiffness composite plates. *Composite Structures*, 98:34–46, April 2013.

[24] Z. Gürdal, B.F. Tatting, and C.K. Wu. Variable stiffness composite panels: Effects of stiffness variation on the in-plane and buckling response. *Composites Part A: Applied Science and Manufacturing*, 39(5):911–922, May 2008.

[25] Z. Gürdal and Reynaldo Olmedot. In-Plane Response of Laminates with Spatially Varying Fiber Orientations : Variable Stiffness Concept. 31(4), 1993.

[26] Chris Waldhart, Calvin Ribbens, and Robert M Jones. Analysis of Tow-Placed , Variable-Stiffness Laminates Design of Tow-Placed , Variable-Stiffness Laminates. 1996.

[27] Jose Reinoso, Roozbeh Nabavi, Raimund Rolfes, and E. L. Jansen. Thermo-mechanical bowing of silicon solar cells during the production procedure. pages 24–26, 2013.

[28] Marie-laure Dano. SMA-Induced Deformations in General Unsymmetric Laminates SMA-Induced Deformations in General Unsymmetric Laminates. 1997.